Cantor set model of eolian dust deposits on desert alluvial fan terraces

Jon D. Pelletier*
Department of Geosciences, University of Arizona, Gould-Simpson Building, 1040 East Fourth Street, Tucson, Arizona 85721–0077, USA

ABSTRACT

Available data show that eolian dust accumulation rates on desert alluvial fan terraces are often inversely proportional to the square root of the terrace age for a given area. This temporal scaling is similar to that observed in fluvial and marine stratigraphic sequences in which a fractal distribution of hiatuses occurs (i.e., a Cantor set). Eolian dust accumulation on alluvial fan terraces is controlled by regional climatic influences on dust deposition (e.g., dessication of pluvial lakes in the early Holocene) and local surface characteristics (e.g., vegetation and pavement coverage) that control dust preservation. In order to interpret the observed scaling in terms of these relative influences I consider two end-member models: (1) a deterministic model in which dust deposition is controlled by cyclical climatic changes (i.e., glacial-interglacial cycles) and in which no erosion occurs, and (2) a stochastic model in which erosion and deposition take place with equal probability and magnitude during each time step (i.e., a bounded random walk). The observed temporal scaling is most consistent with the bounded random walk model, suggesting that long-term eolian dust accumulation is predominantly controlled by episodic changes in vegetation and pavement coverage over time and that eolian dust deposits are strongly punctuated by episodes of erosional reworking at a wide range of temporal scales.

Keywords: eolian, dust, alluvial fan, soils, mathematical model.

INTRODUCTION

Eolian dust accumulation plays an important role in controlling the hydrology, pedology, and ecology of alluvial fan terraces (Yaalon and Ganor, 1973; McFadden et al., 1987; Chadwick and Davis, 1990). The input of fine silt and clay particles into gravelly parent material, for example, can reduce soil hydrologic conductivities by a factor of 100 over geologic time scales (Young et al., 2004). Dust accumulation also controls calcium carbonate development in many aridic soils, which in turn can influence the types of vegetation that grow on them (McAuliffe, 1994). As such, eolian dust accumulation has been a central focus of surface-process studies in the arid and semiarid southwestern U.S. (e.g., McFadden et al., 1987; Reheis et al., 1995).

Dust accumulation on desert alluvial fan terraces can be affected by changes in either deposition or erosion. Previous studies have argued that climatically controlled dust deposition plays the predominant role in controlling dust accumulation on alluvial fan terraces, implicitly assuming that erosion was either negligible or constant on geologic time scales. Low rates of long-term (10^5–10^6 yr) dust accumulation in the southwestern U.S., for example, have been interpreted as a direct result of low dust deposition during the predominantly cool, wet Pleistocene, whereas high rates of shorter-term (10^3–10^4 yr) dust accumulation have been interpreted as an early Holocene pulse of dust deposition related to pluvial lake dessication (Chadwick and Davis, 1990; Reheis et al., 1995; McFadden et al., 1986, 1998). In this paper I compare the observed eolian silt accumulation rates at six alluvial fan study sites with the predictions of quantitative models for eolian dust accumulation to test whether regional climatic controls on dust deposition or the effects of local surface coverage on dust preservation are most important for dust accumulation.

DATA ANALYSIS

Reheis et al. (1995) synthesized data on eolian dust accumulation from alluvial fan terrace study sites in the southwestern U.S. with optimal age control. These sites are located on gently sloping, planar alluvial fan terraces that have not been subject to flooding since abandonment by fan-head entrenchment. This time since fan-head entrenchment is the surface age, and it corresponds to the time interval of eolian dust accumulation. Figure 1 plots silt accumulation rates versus time interval on logarithmic scales for these locations. Error bars represent time interval (i.e., surface age) uncertainties. All of the locations studied by Reheis et al. (1995) that have at least four data points (i.e., distinct alluvial fan terraces) have been included. The plots in Figure 1 (A–D) exhibit a power-law trend (i.e., a straight line on log-log scales) given by

$$R \propto T^{-\alpha}, \quad (1)$$

where R is the accumulation rate, T is the time interval of accumulation, and α is an exponent close to 0.5. Values of α for each data set were obtained by a linear fit of the logarithm of accumulation rate to the logarithm of time interval, weighted by the age uncertainty for each point. Accumulation rates plotted in Figures 1E and 1F (lower and upper fans near Silver Lake Playa) show only a weak dependence on time interval. Figure 1E, for example, has a nearly constant rate across time intervals, while Figure 1F shows a peak in accumulation rates at time intervals of 10^3–10^4 yr, consistent with an early Holocene dust pulse. Although only silt accumulations are plotted in Figure 1 (except for Fig. 1C, which gives results for clay accumulation on the Whipple Mountains fan because silt data were not available), results for clay and salt fractions at the same locations were broadly similar.

MODEL DESCRIPTION

In order to interpret the temporal scaling of dust accumulation rates with time interval I considered two end-member models. The first model assumes that the magnitude of dust deposition and erosion is constant through time (with a rate equal to 0.01 g/cm^2/yr in this example) and that erosion or deposition takes place with equal probability during each time step (1 yr). Figure 2A illustrates two runs of this bounded random walk model. The walk is bounded because the net accumulation is always positive (in an unbounded random walk, negative values are also allowed). At the longest time interval (~10^4 yr), both model runs have accumulated ~1.5 g/cm^2 of dust (equal to a thickness of 1.5 cm if a density of 1 g/cm^3 is assumed).

*E-mail: jdpellet@email.arizona.edu.

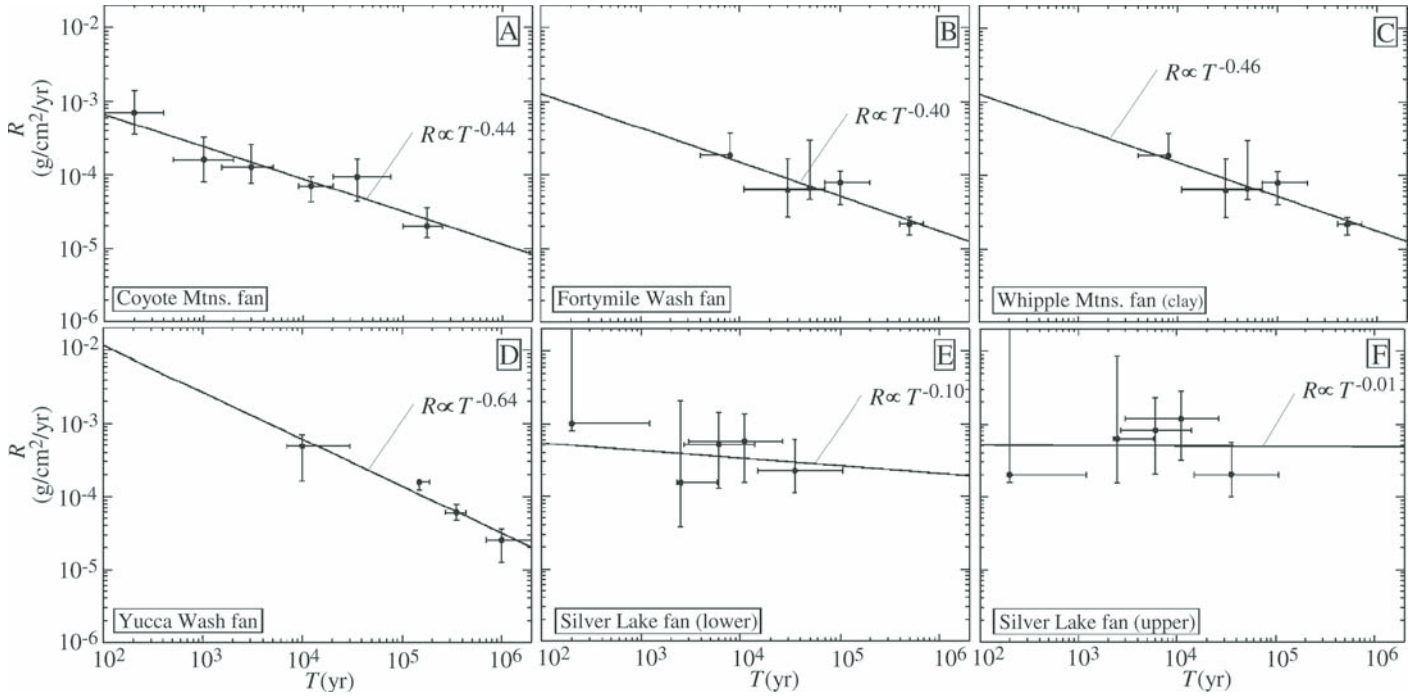

Figure 1. Plots of silt accumulation rates (*R*) vs. time interval (*T*) on alluvial fan terrace surfaces (from data in Reheis et al., 1995). A: Coyote Mountains fan. B: Fortymile Wash fan. C: Whipple Mountains fan (clay fraction shown). D: Yucca Wash fan. E: Lower fan near Silver Lake Playa. F: Upper fan near Silver Lake Playa. Best-fit lines indicate power-law scaling with exponents close to –0.5 for A–D. Trends in E and F are more consistent with linear accumulation or cyclical climate models.

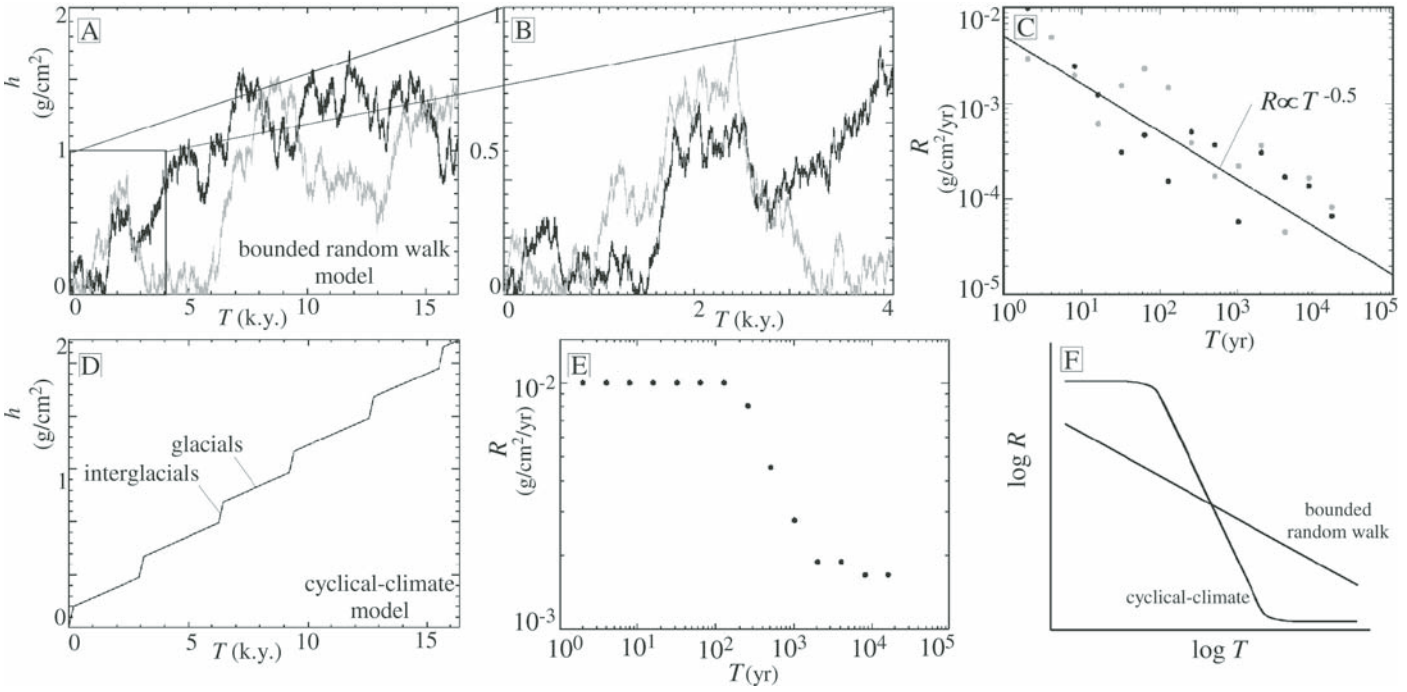

Figure 2. A: Plot of dust accumulation vs. time for two runs of bounded random walk model. B: Inset of A illustrating scale-invariance of bounded random walk model by rescaling time by factor of 4 and accumulation by factor of 2. C: Plot of accumulation rate vs. time interval illustrating power-law scaling behavior. D: Plot of dust accumulation vs. time in cyclical climate model. E: Plot of accumulation rate vs. time interval in cyclical-climate model, illustrating inverted S-shaped curve. F: Schematic diagram summarizing results of two models for accumulation rate vs. time interval.

On shorter time intervals (10^3 and 10^2 yr), net accumulations are smaller than the 1.5 value, but they are not linearly proportional to the time interval. For example, net accumulation is 0.3–0.5 g/cm^2 over 10^3 yr for the two model runs shown, a much larger change per unit time than the 1.5 g/cm^2 observed over 10^4 yr. Figure 2B illustrates the temporal scaling of accumulation rates versus time interval in this model. The results in Figure 2B illustrate that accumulation rates decrease, on average, at a rate proportional to one over the square root of the time interval, similar to that in Figures 1A–1D.

This power-law scaling behavior can also be derived theoretically. The average distance from zero in a bounded random walk, $\langle h \rangle$, increases with the square root of the time interval, T (van Kampen, 2001):

$$\langle h \rangle = aT^{1/2}, \quad (2)$$

where the brackets denote the value that would be obtained by averaging the result of many different model runs and a is the magnitude of erosion or deposition during each time step. As applied to eolian dust accumulation, the average distance $\langle h \rangle$ represents the total accumulation of eolian dust (in g/cm^2 or cm) on the surface, including the effects of episodic erosion. The average accumulation rate is obtained by dividing equation 2 by T to give

$$\langle R \rangle = aT^{-1/2}. \quad (3)$$

While the average rate scales according to equation 3, individual runs of the bounded random walk model do not follow equation 3 exactly due to fluctuations inherent in the model.

In the second end-member model, dust deposition is assumed to have a high value during interglacial periods (0.01 g/cm^2/yr), a low value during glacial periods (0.002 g/cm^2/yr), and no erosion. Figure 2E illustrates the accumulation rate versus time interval for this model. The plot follows an inversed S-shaped curve (Fig. 2E). This relationship is characteristic of accumulation rate curves for all periodic functions (Sadler and Strauss, 1990), and it is markedly different from the observed scaling in Figures 1A–1D.

The scaling behavior of accumulation rates shown in Figures 1A–1D is broadly similar to that observed in fluvial and marine deposits, and has a close association with the problem of stratigraphic completeness. Fluvial and marine stratigraphic sections are often incomplete because unconformities or hiatuses with a broad distribution of time intervals are present in these sections (Sadler, 1981). The accumulation rate curve can be used to quantify the completeness of a given section using the ratio of the overall accumulation rate to the average rate at a particular time interval T (Sadler and Strauss, 1990). In the bounded random walk model, for example, a complete stratigraphic section (i.e., one with no hiatuses) of 10 k.y. duration would have a total accumulation of 100 g/cm^2 based on an annual accumulation rate of 0.01 g/cm^2. The bounded random walk model, in contrast, has an average accumulation of 1 g/cm^2 over 10 k.y. based on equation 2. Therefore, a 10 k.y. sequence is only 1% complete (i.e., 99% of the mass that was once deposited has been eroded). Plotnick (1986) showed that a power-law accumulation-rate curve (i.e., equation 1) specifically implied a power-law or fractal distribution of hiatuses, with few hiatuses of very long duration and many of short duration, analogous to the Gutenberg-Richter power-law distribution of earthquake magnitudes (Turcotte, 1997).

To see how temporal scaling of accumulation rates relates to the completeness of the stratigraphic record and to a fractal distribution of hiatuses, consider the accumulation model illustrated in Figures 3A–3C (after Plotnick, 1986). Depositional units (beds) in this model are of equal thickness. The depth of each bed is given as a function of age in Figure 3A. The time intervals of preserved deposits are characterized by a second-order Cantor set. A Cantor set is a classic fractal pattern created by repeatedly deleting the middle thirds from a set of line segments, starting by deleting the middle third of the line segment [0,1] to leave [0,1/3] and [2/3,1] (i.e., a first-order Cantor set). Next the middle thirds of these two remaining line segments are removed to create a second-order Cantor set. Mathematically, a true Cantor set is created when this process of removing middle thirds is continued ad infinitum, but in nature there is always a finite bed thickness that limits the fractal scaling. Figure 3A shows that at the largest time interval (9 yr), 8 mm of sediments have accumulated, so the mean rate of accumulation is R (9 yr) = 8 mm/9 yr = 0.89 mm/yr over this period. Similarly, during the first three years of accumulation the mean rates of accumulation are R (3 yr) = 4 mm/3 yr = 1.33 mm/yr. Thus the rate of deposition increases as the period considered decreases. This is shown in Figure 3B, where the power-law temporal scaling is illustrated. The bounded random walk model leads to a stochastic rather than a deterministic Cantor set, and to an exponential distribution of bed thicknesses rather than a single uniform bed thickness (Pelletier and Turcotte, 1997). Figure 3D illustrates the chronostratigraphic plot corresponding to a single run of the bounded random walk model (with a = 0.01 cm/yr) shown in Figure 3C. In this plot, sediments deposited that are later eroded are removed from the sequence and identified as horizontal lines (hiatuses). The bounded random walk model results in a fractal distribution of hiatus lengths, located randomly in the domain, and exhibits power-law scaling of accumulation rate versus time interval similar to the deterministic Cantor set of Figures 3A and 3B.

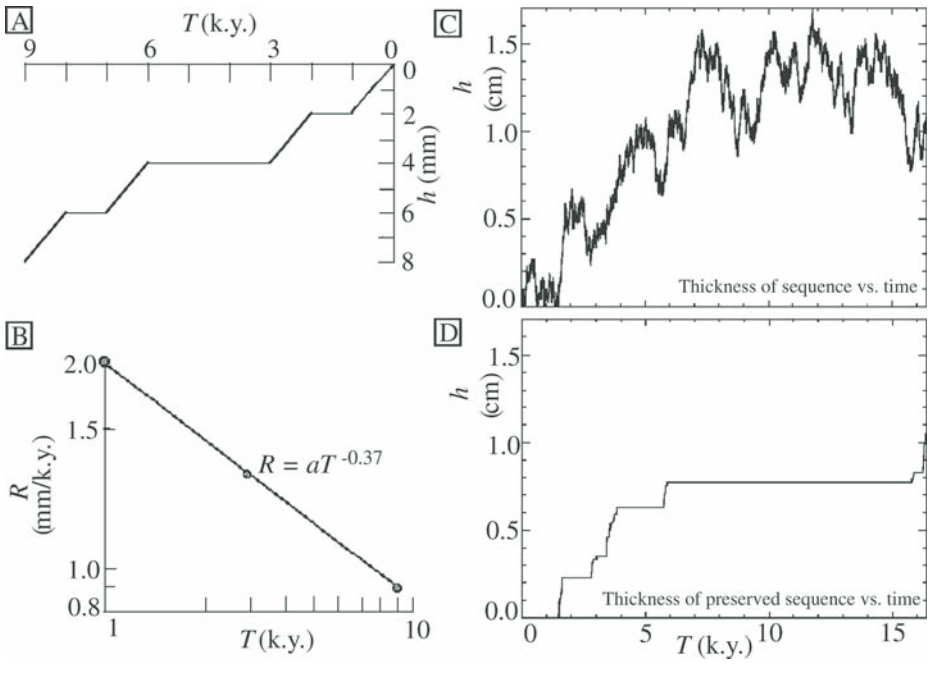

Figure 3. A, B: Illustration of synthetic stratigraphic section based on second order Cantor set. A: Depth of sediments *h* (mm) as function of sediment age (k.y.). B: Accumulation rate *R* as function of time interval *T* for model stratigraphic section in A. C: Plot of accumulation *h* (cm) in bounded random walk model as function of time assuming *a* = 0.01 cm/yr (*a* is magnitude of erosion or deposition during each time step). D: Chronostratigraphic plot of C, in which all sediment later eroded has been removed to indicate hiatuses (horizontal lines).

DISCUSSION AND CONCLUSIONS

Temporal scaling of accumulation rates in the bounded random walk model is observed down to time scales as low as the time step at which erosion and deposition alternate randomly. The success of this model in reproducing the observed temporal scaling of eolian accumulation rates suggests that erosion and deposition alternate over time scales $<\sim 10^2$–10^3 yr based on the lower limit of observed scaling in Figures 1A–1D. What process or processes could result in erosional and depositional alternation at time scales of 10^2–10^3 yr or smaller? Vegetation growth and decay is a likely possibility, either at the plant scale during individual births and deaths or at the landscape scale during interannual climatic changes. The presence of shrubs, for example, generally protects the nearby ground from eolian erosion and promotes deposition (Wolfe and Nickling, 1993). When a plant dies and its cover is removed, however, the ground surface is often mounded and susceptible to local wind erosion (Whicker et al., 2002). In such cases the fundamental time scale for alternation could be either the mean shrub lifespan, which is typically $\sim 10^2$ yr (Cody, 2000), or at the interannual and interdecadal time scales of short-term climatic changes that modulate landscape-scale vegetation cover.

The results of Figure 1 suggest that eolian dust accumulation on alluvial fans located close to playa sources (Figs. 1E, 1F) is fundamentally different from that on fans located far from playa sources (Fig. 1A–1D). The fan study sites close to Silver Lake Playa exhibit a linear accumulation trend on the lower fan site and a cyclical climate trend on the upper fan site while the remaining fan sites exhibit accumulation trends consistent with the bounded random walk model. This distinction between fans proximal and distal to playa sources is consistent with the results of Pelletier and Cook (2005), who showed that dust accumulation is strongly localized downwind from playa sources and decreases to regional background values within a few kilometers from a playa source. The results of Figure 1 and those of Pelletier and Cook (2005) suggest that the bounded random walk model may be representative of the majority of fans located far (i.e., greater than a few kilometers) from playas, and that the classic linear-accumulation or cyclical-climate models are representative of accumulation on fans proximal to playa sources where dust deposition is rapid enough to overwhelm the effects of episodic disturbances.

Climate cannot be dismissed as a factor in dust accumulation, and it cannot be argued that dust accumulation on desert surfaces is purely random. It is clear from ice core records that global dust deposition varies strongly with glacial-interglacial cycles (Petit et al., 1990), and such variations must have an influence on dust accumulation. It is also clear that dust accumulation is not purely a random process. Dust accumulation and desert pavements, for example, clearly coevolve by a positive feedback in which dust accumulation promotes clast migration and suturing through wetting-drying cycles, thereby increasing dust preservation in a positive feedback (McFadden et al., 1987). Nevertheless, the results shown in this paper suggest that eolian deposits preserve only a tiny fraction of the total dust deposited on the surface over time. Care should be taken, therefore, in interpreting eolian dust deposits in terms of purely deterministic factors.

ACKNOWLEDGMENTS

I thank Peter Sadler and Marith Reheis for helpful reviews, and the U.S. Army Research Office Terrestrial Sciences Program (grant W911NF-04-1-0266) for financial support. This work would not have been possible without the painstaking effort of many U.S. Geological Survey geologists, especially Reheis, over the course of many years.

REFERENCES CITED

Chadwick, O.A., and Davis, J.O., 1990, Soil-forming intervals caused by eolian sediment pulses in the Lahontan basin, northwestern Nevada: Geology, v. 18, p. 243–246, doi: 10.1130/0091–7613(1990)018<0243:SFICBE>2.3.CO;2.

Cody, M.L., 2000, Slow-motion population dynamics in Mojave Desert perennial plants: Journal of Vegetation Science, v. 11, p. 351–358.

McAuliffe, J.R., 1994, Landscape evolution, soil formation, and ecological patterns and processes in Sonoran Desert bajadas: Ecological Monographs, v. 64, p. 111–148, doi: 10.2307/2937038.

McFadden, L.D., Wells, S.G., and Dohrenwend, J.C., 1986, Influences of Quaternary climatic changes on processes of soil development on desert loess deposits of the Cima volcanic field, California: Catena, v. 13, p. 361–389, doi: 10.1016/0341–8162(86)90010-X.

McFadden, L.D., Wells, S.G., and Jercinovich, M.J., 1987, Influences of eolian and pedogenic processes on the origin and evolution of desert pavements: Geology, v. 15, p. 504–508, doi: 10.1130/0091–7613(1987)15<504:IOEAPP>2.0.CO;2.

McFadden, L.D., McDonald, E.V., Wells, S.G., Anderson, K., Quade, J., and Forman, S.L., 1998, The vesicular layer and carbonate collars of desert soils and pavements: Formation, age, and relation to climate change: Geomorphology, v. 24, p. 101–145, doi: 10.1016/S0169–555X(97)00095–0.

Pelletier, J.D., and Cook, J.P., 2005, Deposition of playa windblown dust over geologic time scales: Geology, v. 33, p. 909–912, doi: 10.1130/G22013.1.

Pelletier, J.D., and Turcotte, D.L., 1997, Synthetic stratigraphy with a stochastic diffusion model of sedimentation: Journal of Sedimentary Research, v. 67, p. 1060–1067.

Petit, J.R., Mounier, M., Jouzel, J., Korotkevitch, Y., Kotlyakov, V., and Lorius, C., 1990, Paleoclimatological implications of the Vostok core dust record: Nature, v. 343, p. 56–58, doi: 10.1038/343056a0.

Plotnick, R.E., 1986, A fractal model for the distribution of stratigraphic hiatuses: Journal of Geology, v. 94, p. 885–890.

Reheis, M.C., Goodmacher, J.C., Harden, J.W., McFadden, L.D., Rockwell, T.K., Shroba, R.R., Sowers, J.M., and Taylor, E.M., 1995, Quaternary soils and dust deposition in southern Nevada and California: Geological Society of America Bulletin, v. 107, p. 1003–1022, doi: 10.1130/0016–7606(1995)107<1003:QSADDI>2.3.CO;2.

Sadler, P.M., 1981, Sediment accumulation rates and the completeness of stratigraphic sections: Journal of Geology, v. 89, p. 569–584.

Sadler, P.M., and Strauss, D.J., 1990, Estimation of completeness of stratigraphic sections using empirical data and theoretical models: Geological Society [London] Journal, v. 147, p. 471–485.

Turcotte, D.L., 1997, Fractals and chaos in geology and geophysics: New York, Cambridge University Press 398 p.

van Kampen, N.G., 2001, Stochastic processes in physics and chemistry: Amsterdam, Elsevier, 419 p.

Whicker, J.J., Breshears, D.D., Wasiolek, P.T., Kirchner, T.B., Tavani, R.A., Schoep, D.A., and Rodgers, J.C., 2002, Temporal and spatial variation of episodic wind erosion in unburned and burned semiarid shrubland: Journal of Environmental Quality, v. 31, p. 599–612.

Wolfe, S.A., and Nickling, W.G., 1993, The protective role of sparse vegetation in wind erosion: Progress in Physical Geography, v. 17, p. 50–68.

Yaalon, D.H., and Ganor, E., 1973, The influence of dust on soils in the Quaternary: Soil Science, v. 116, p. 146–155, doi: 10.1097/00010694–197309000–00003.

Young, M.H., McDonald, E.V., Caldwell, T.C., Benner, S.G., and Meadows, D.G., 2004, Hydraulic properties of a desert soil chronosequence, Mojave Desert: CA: Vadose Zone Journal, v. 3, p. 956–963.

Manuscript received 15 September 2006
Revised manuscript received 21 December 2006
Manuscript accepted 28 December 2006

Printed in USA